Topology in Superposition

Wojciech H. Zurek

C. Jess Riedel, REDUNDANT INFORMATION AND THE QUANTUM-CLASSICAL TRANSITION this WEDNESDAY 2 pm in 3302 Broida, a conference room directly across from the elevators on the 3rd floor of the physics building.

- Phase winding by Bose-Einstein condensation
- Miscibility-immiscibility quantum phase transition
- Critical dynamics of decoherence
- Assisted finite rate adiabatic passage through quantum critical point
- Topological Schrödinger Cat in a quantum Ising chain
- Quench from Mott insulator to superfluid

Phase winding around the loop…

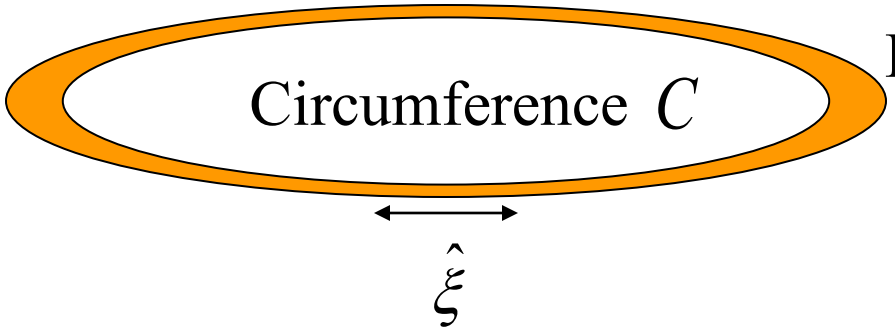

Phase chosen independently in each of $N = C/\hat{\xi}$ fragments of the loop

Therefore, expected mismatch of phase of the "condensate" is:

$$\Delta\theta = \sqrt{N} = \sqrt{\frac{C}{\hat{\xi}}}$$

This implies a gradient of phase of $\Delta\theta / C$ which implies a velocity:

$$v = \frac{\mathsf{h}}{m}\frac{\sqrt{N}}{C}$$

and a **winding number:**

$$w = \frac{\Delta\theta}{2\pi} = \frac{\sqrt{N}}{2\pi}$$

(WHZ, Nature '85)

In a loop topology winding number is preserved.

First experiment: Polturak et al., Haifa, 2001… More recent experiments by Brian Anderson, Tucson:

"When symmetry breaks, how big are the pie

All second order phase transitions fall into **universality classes** characterized by the behavior of quantities such as specific heat, magnetic susceptibility, etc. This is also the case for quantum phase transitions.

Equilibrium behavior of the **relaxation time** and of the **healing length** near the **critical point** will be essential; they **determine density of topological defects formed by nonequilibrium phase transition -- by "the quench".**

"CRITICAL SLOWING DOWN"

$$\tau = \frac{\tau_0}{|\varepsilon|}$$

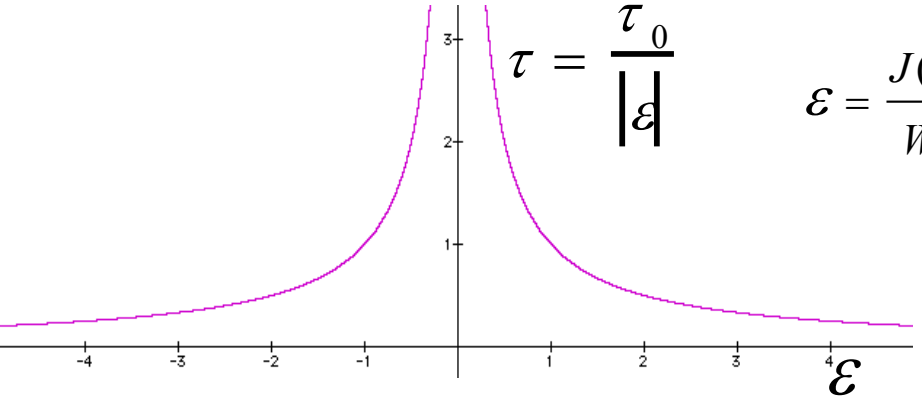

$$\varepsilon = \frac{J(t)}{W} - 1 = \frac{T}{T_C} - 1$$

"CRITICAL OPALESCENCE"

$$\xi = \frac{\xi_0}{\sqrt{|\varepsilon|}}$$

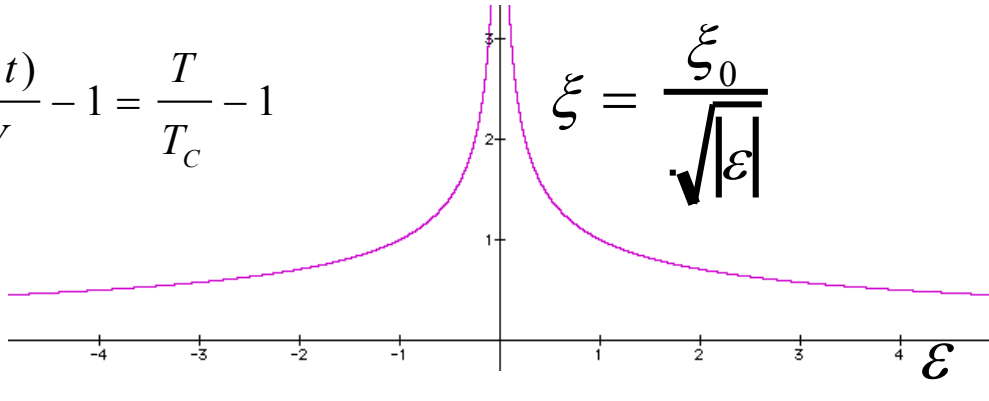

Derivation of the "freeze out time"…

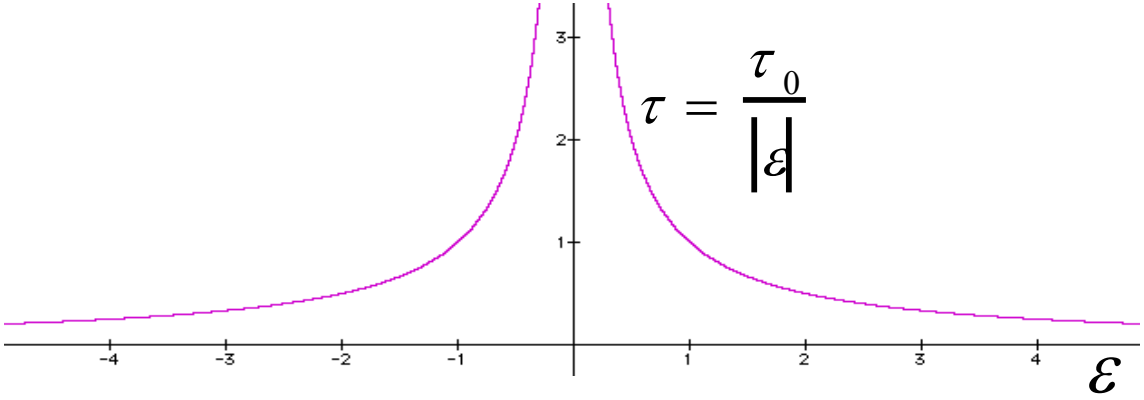

Assume:

$$\varepsilon = \frac{time}{"quench \quad time"} = \frac{t}{\tau_Q}$$

Relaxation time:

$$\tau = \frac{\tau_0}{|\varepsilon|}$$

determines "reflexes" of the system.

The potential $V_{Ginzburg-Landau}(\varphi) = \varepsilon|\varphi|^2 + |\varphi|^4$ changes at a rate given by:

$$\frac{\varepsilon}{\dot{\varepsilon}} = t$$

Relaxation time is equal to this rate of change when $\tau(\varepsilon(\hat{t})) = \hat{t}$

… and the corresponding "frozen out" healing length $\hat{\xi}$

….. $\tau(\varepsilon(\hat{t})) = \hat{t}$

Hence: $\tau_0 / (\hat{t} / \tau_Q) = \hat{t}$

Or:

$$\hat{t} = \sqrt{\tau_0 \tau_Q} \;\&\; \hat{\varepsilon} = \sqrt{\tau_0 / \tau_Q}$$

The corresponding length follows:

$$\hat{\xi} = \xi_0 / \sqrt{\hat{\varepsilon}} = \xi_0 \sqrt[4]{\frac{\tau_Q}{\tau_0}}$$

$$\hat{\xi} = \xi_0 \left| \tau_Q / \tau_0 \right|^{\nu/(1+\nu z)}$$

WHZ, Nature, 317, 505 (1985)…

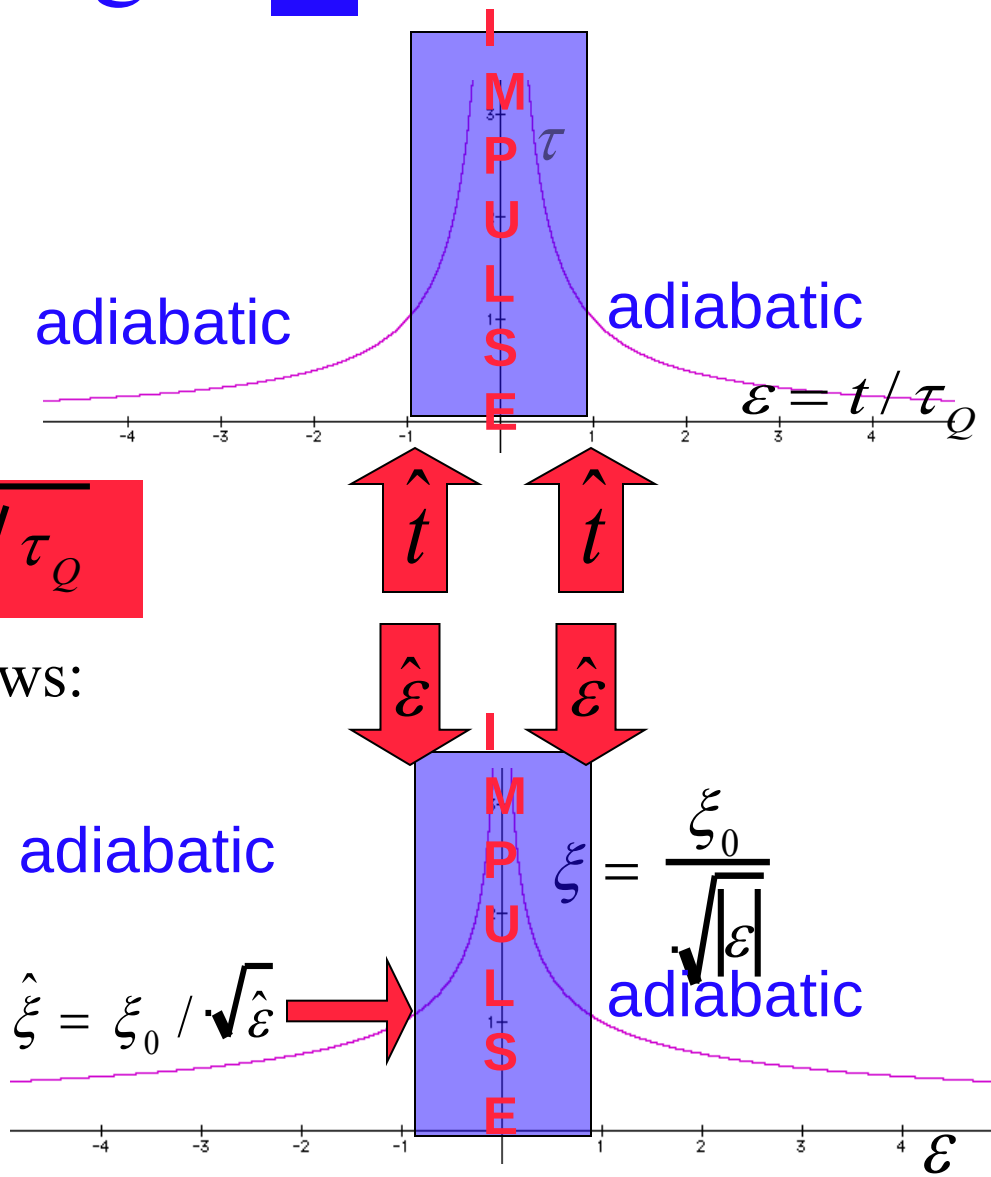

Our simulation of Bose-Einstein condensatio in a torus:

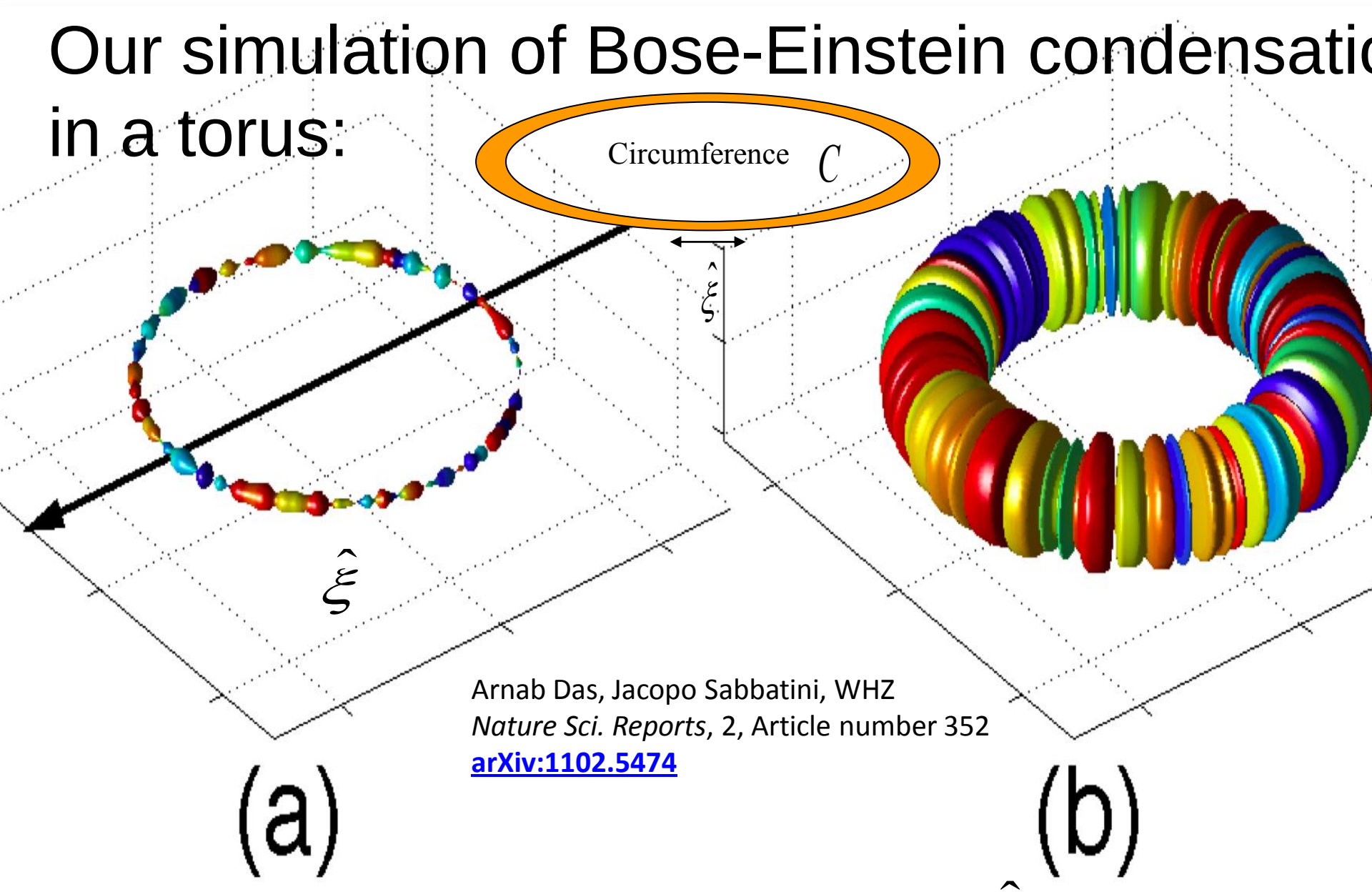

Arnab Das, Jacopo Sabbatini, WHZ
Nature Sci. Reports, 2, Article number 352
arXiv:1102.5474

When symmetry breaks, how can one calculate $\hat{\xi}$, the "size of the pieces"?

We consider a BEC in a quasi-1D ring of circumference C, an idealization of quasi-1D toroidal geometry, e.g., see [12–14]. We model it using the stochastic Gross-Pitaevskii equation (SGPE) [22]:

$$(i-\gamma)\frac{\partial\phi}{\partial t} = -\frac{1}{2}\frac{\partial^2\phi}{\partial x^2} + \epsilon(t)\phi + \tilde{g}|\phi|^2\phi + \eta(x,t), \quad (1)$$

where $\phi = |\phi(x)|e^{i\theta(x)}$ is the condensate wavefunction and $\eta(x,t)$ is the thermal noise satisfying the fluctuation-dissipation relation $\langle\eta(x,t)\eta^*(x',t')\rangle = 2\gamma T\delta(x-x')\delta(t-t')$, with γ representing the dissipation, T the noise temperature, $\tilde{g}$ the non-linearity parameter and $-\epsilon$ the chemical potential [21]. Leaving aside the noise and dissipation, the above system can be described by the energy functional $\mathcal{E} = \oint_{ring}[\frac{1}{2}|\partial_x\phi|^2 + U(|\phi|)]dx$, where $U(|\phi|) = \epsilon|\phi|^2 + \frac{1}{2}\tilde{g}|\phi|^4$. Extremizing the energy functional we obtain $\phi = 0$ for $\epsilon > 0$ and $\phi = \sqrt{|\epsilon|/\tilde{g}}\exp(i\theta)$ for $\epsilon < 0$, where θ is the wave function phase ($\epsilon = 0$ is the critical point). We induce the transition by quenching ϵ:

$$\epsilon(t) = -t/\tau_Q \quad (2)$$

from an initial $\epsilon > 0$ to a final $\epsilon < 0$, and allow the system enough time to thermalize initially and stabilize eventually [23]. The critical point is crossed at $t_c = 0$.

Winding up superfluid in a torus via Bose Einstein condensation

Arnab Das, Jacopo Sabbatini, Wojciech H. Zurek

Scientific Reports 2, Article #352, (2012) (**arXiv:1102.5474**)

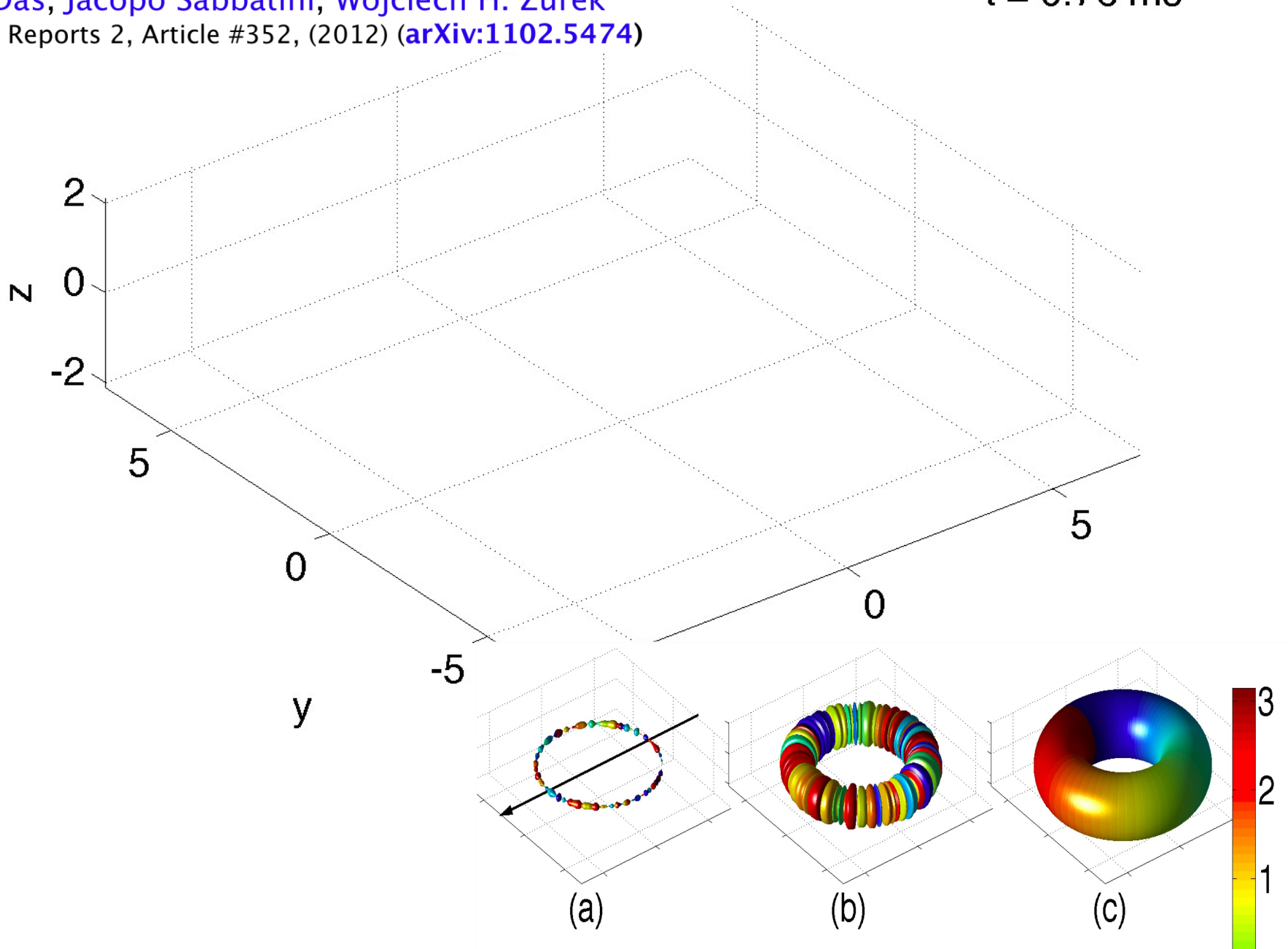

Winding number

Condensed atom #

Angular momentum

Specific ang. mom.

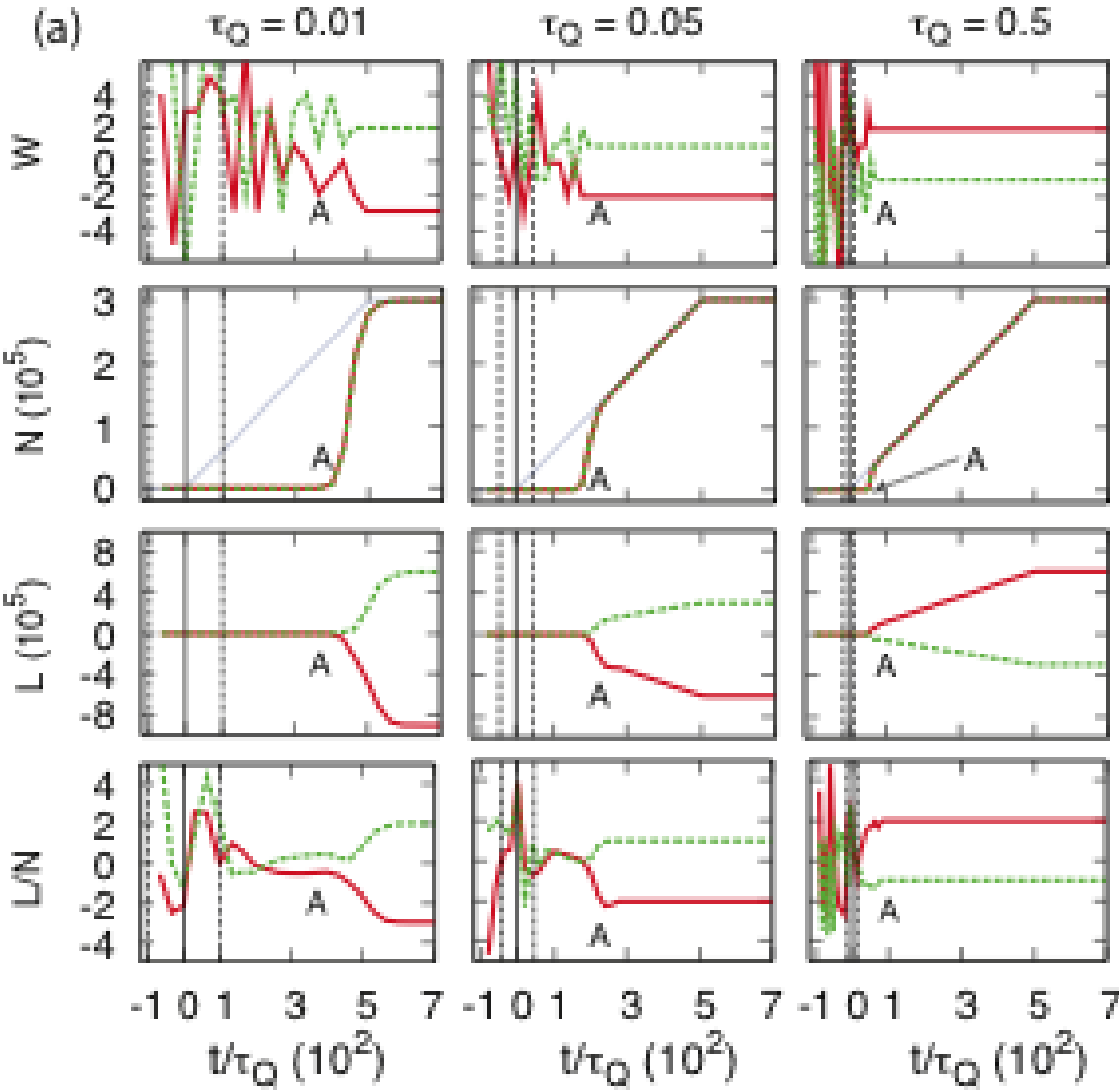

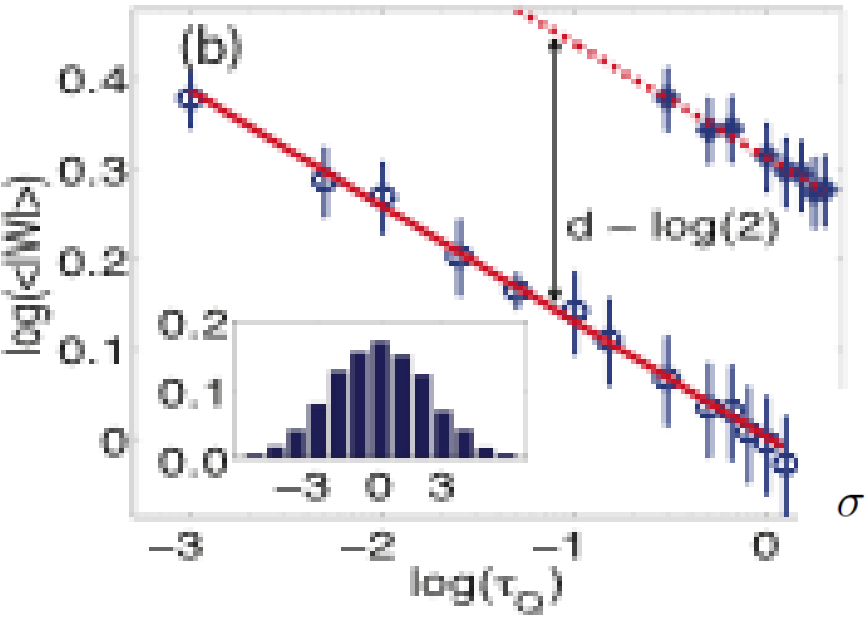

(b) Winding number as a function of quench timescale. (Inset in (b): Distribution of winding numbers For a single quench time is nearly Gaussian.)

$$\hat{\xi} = \xi_0 \left|\tau_Q/\tau_0\right|^{\nu/(1+\nu z)}$$

$$\sigma(W) = \sqrt{\langle W^2 \rangle} = \frac{\tau_0^{1/8}\xi_0^{-1/2}}{2\sqrt{3}} \left(\frac{\sqrt{C}}{\tau_Q^{1/8}}\right) = \sqrt{\frac{\pi}{2}}\langle |W| \rangle$$

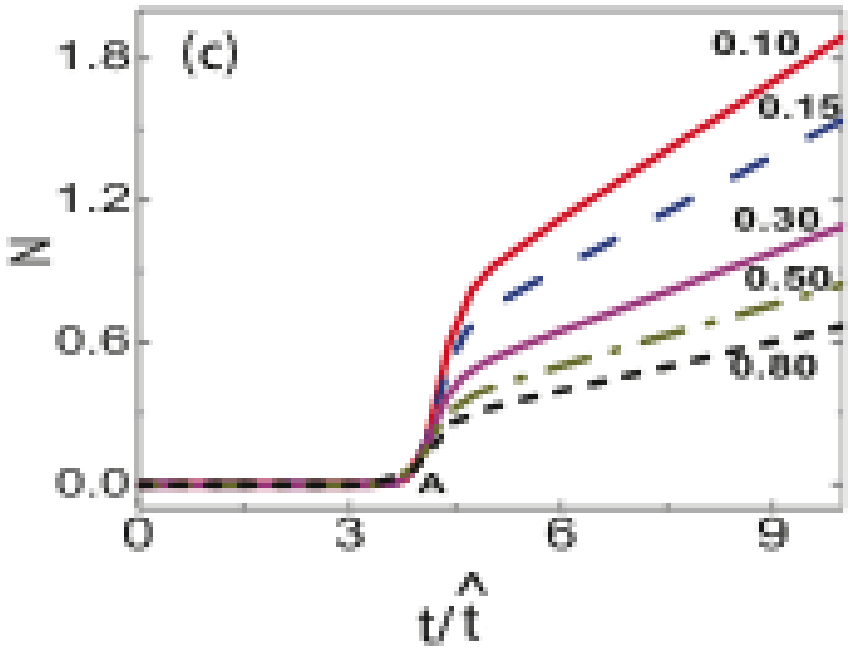

(c) BEC buildup as a function of time lags behind: The critical point is traversed at t=0. All the plots overlap when rescaled by the characteristic time that follows from the KZM:

$$\hat{t} = \left|\tau_0 \tau_Q^{\nu z}\right|^{1/(1+\nu z)}$$

"A" marks sharp "knee" where catching up with equilibrium N starts.

2-D Simulation of BEC Formation

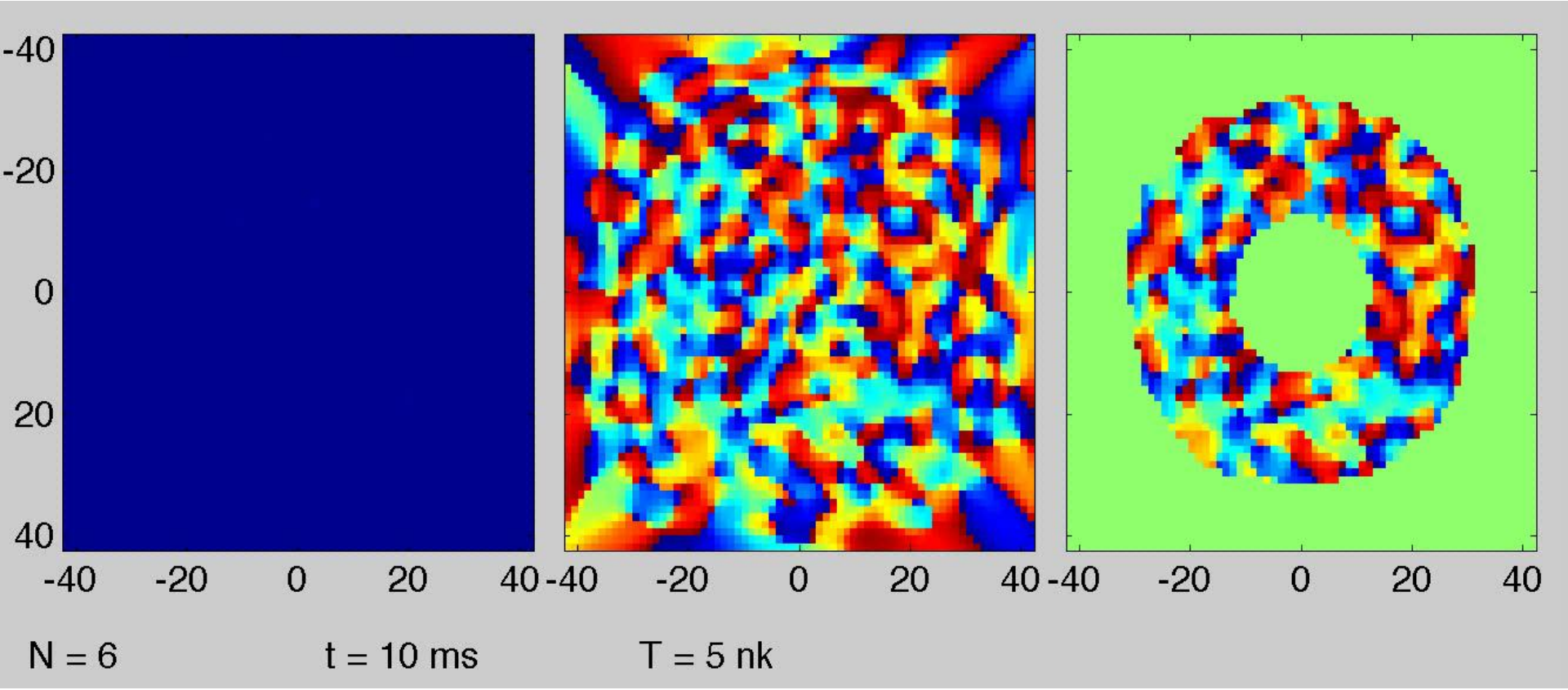

Das, Sabbatini, WHZ

Phase separation and pattern formation in a binary Bose-Einstein condensate

Jacopo Sabbatini,[1,*] Wojciech H. Zurek,[2] and Matthew J. Davis[1]

[1]*The University of Queensland, School of Mathematics and Physics, Qld 4072, Australia*
[2]*Theory Division, Los Alamos National Laboratory, Los Alamos, New Mexico 87545, USA*

(Dated: September 11, 2011)

The miscibility-immiscibility phase transition in binary Bose-Einstein condensates (BECs) can be controlled by a coupling between the two components. Here we propose a new scheme that uses coupling-induced pattern formation to test the Kibble-Zurek mechanism (KZM) of topological-defect formation in a quantum phase transition. For a binary BEC in a ring trap we find that the number of domains forming the pattern scales with the coupling quench rate with an exponent as predicted by the KZM. For a binary BEC in an elongated harmonic trap we find a different scaling law due to the transition being spatially inhomogeneous. We perform a "quantum simulation" of the harmonically trapped system in a ring trap to verify the scaling exponent.

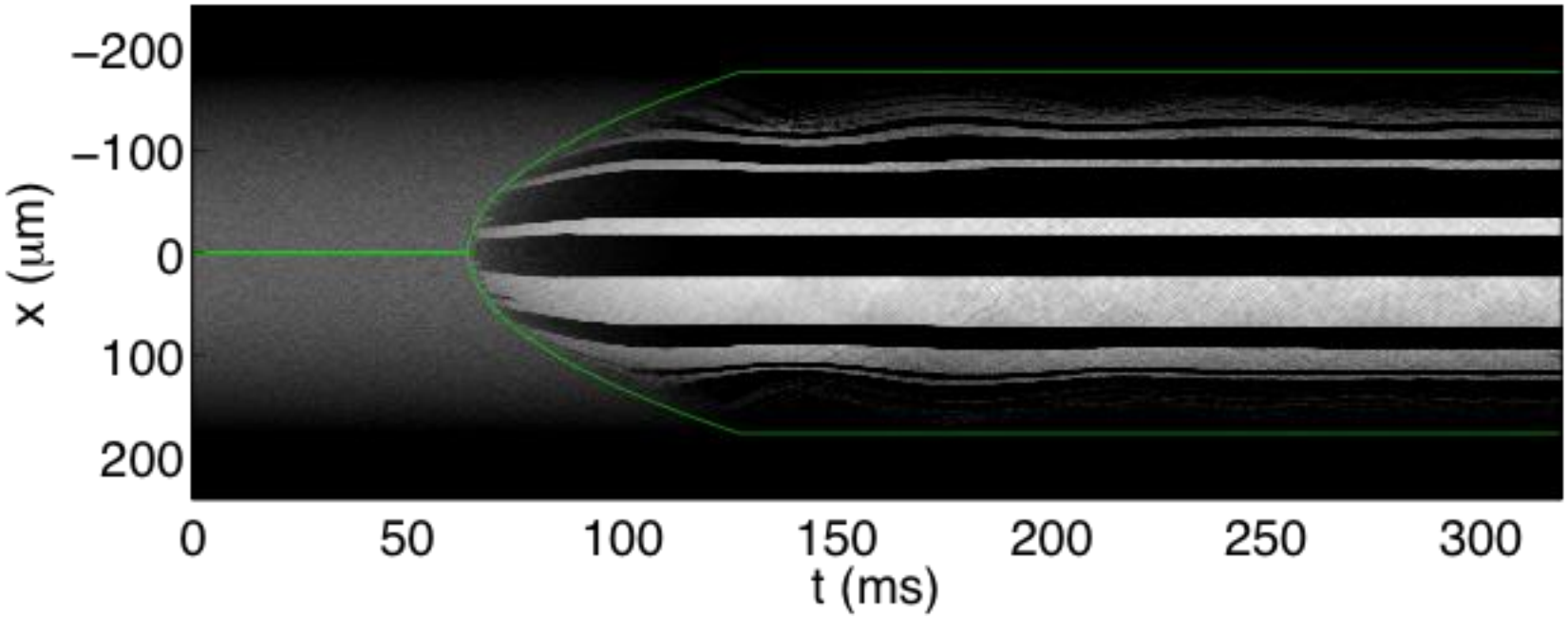

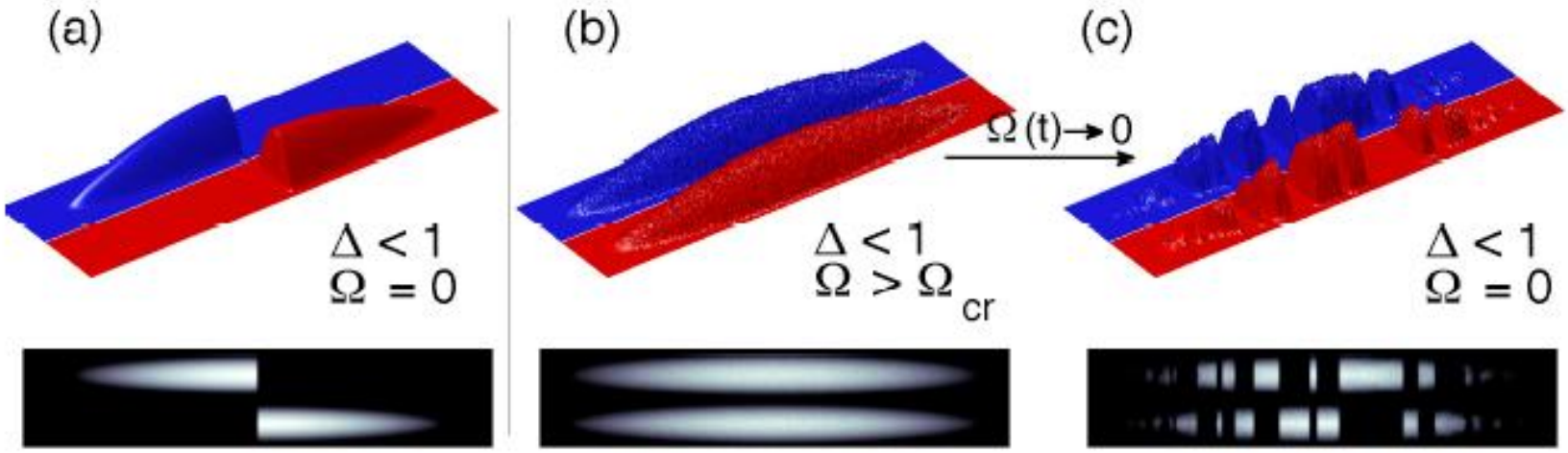

Figure 1. Density of the two components of a binary BEC. (a) Natural ground state of a binary immiscible system. (b) In the strong coupling regime state (a) becomes miscible. Quantum noise has been added that results in the formation of domains (see text). (c) Quenching the coupling $\Omega(t)$ to zero brings the system back to its immiscible phase. If the quench is non-adiabatic a random pattern of domains is created and the system is left in an excited state. We

$$\hat{H}_0 = \int dx \sum_{i=1}^{2} \hat{\psi}_i^\dagger(x) \left[-\frac{\hbar}{2m}\frac{\partial^2}{\partial x^2} + V(x) \right] \hat{\psi}_i(x), \tag{2}$$

$$\hat{H}_{\rm I} = \int dx \left\{ \sum_{i=1}^{2} \left[\frac{g_{ii}}{2} \hat{\psi}_i^\dagger(x)\hat{\psi}_i^\dagger(x)\hat{\psi}_i\hat{\psi}_i(x) \right] + g_{12}\hat{\psi}_1^\dagger(x)\hat{\psi}_2^\dagger(x)\hat{\psi}_2\hat{\psi}_1(x) \right\}, \tag{3}$$

$$\hat{H}_{\rm C} = \int dx \left\{ \hbar\delta\hat{\psi}_2^\dagger(x)\hat{\psi}_2(x) - \hbar\Omega(t)[\hat{\psi}_1^\dagger(x)\hat{\psi}_2(x) + \hat{\psi}_2^\dagger(x)\hat{\psi}_1(x)] \right\}. \tag{4}$$

$$\hat{H} = \hat{H}_0 + \hat{H}_{\rm I} + \hat{H}_{\rm C}$$

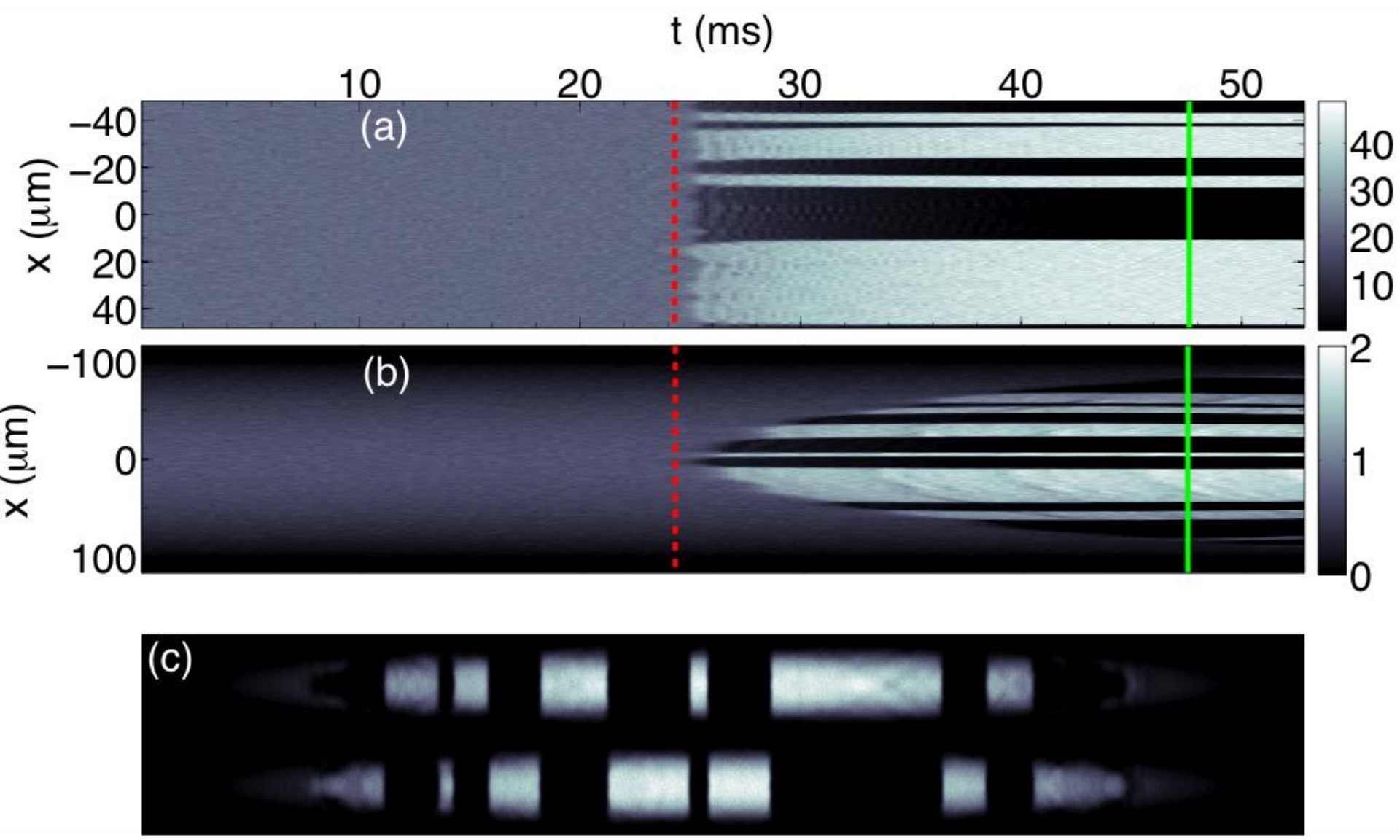

Phase separation and pattern formation in a binary Bose-Einstein condensate

Jacopo Sabbatini, Wojciech H. Zurek, Matthew J. Davis

Phys. Rev. Lett. 107, 230402 (2011) (**arXiv:1106.5843**); NJP, in press

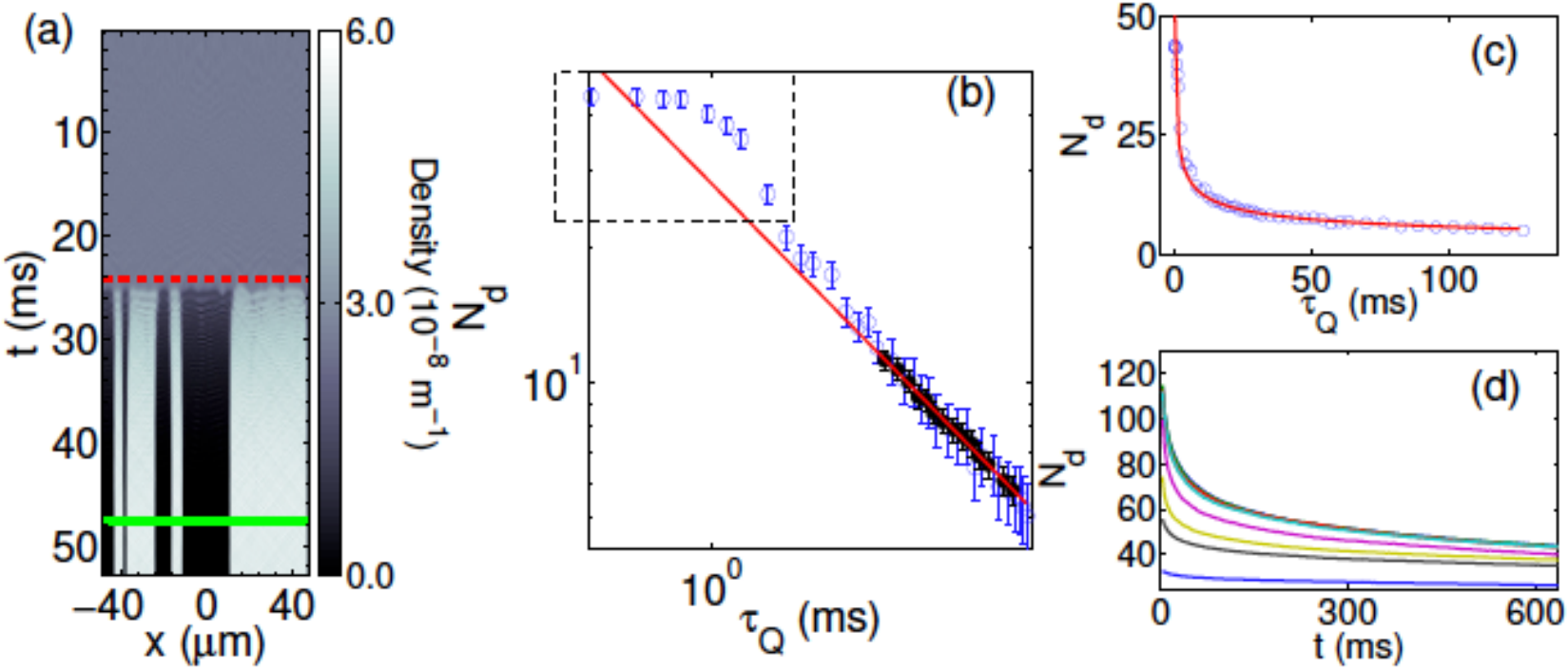
(a)
t (ms)
x (μm)
Density (10^{-8} m^{-1})
(b)
N_d
τ_Q (ms)
(c)
N_d
τ_Q (ms)
(d)
N_d
t (ms)

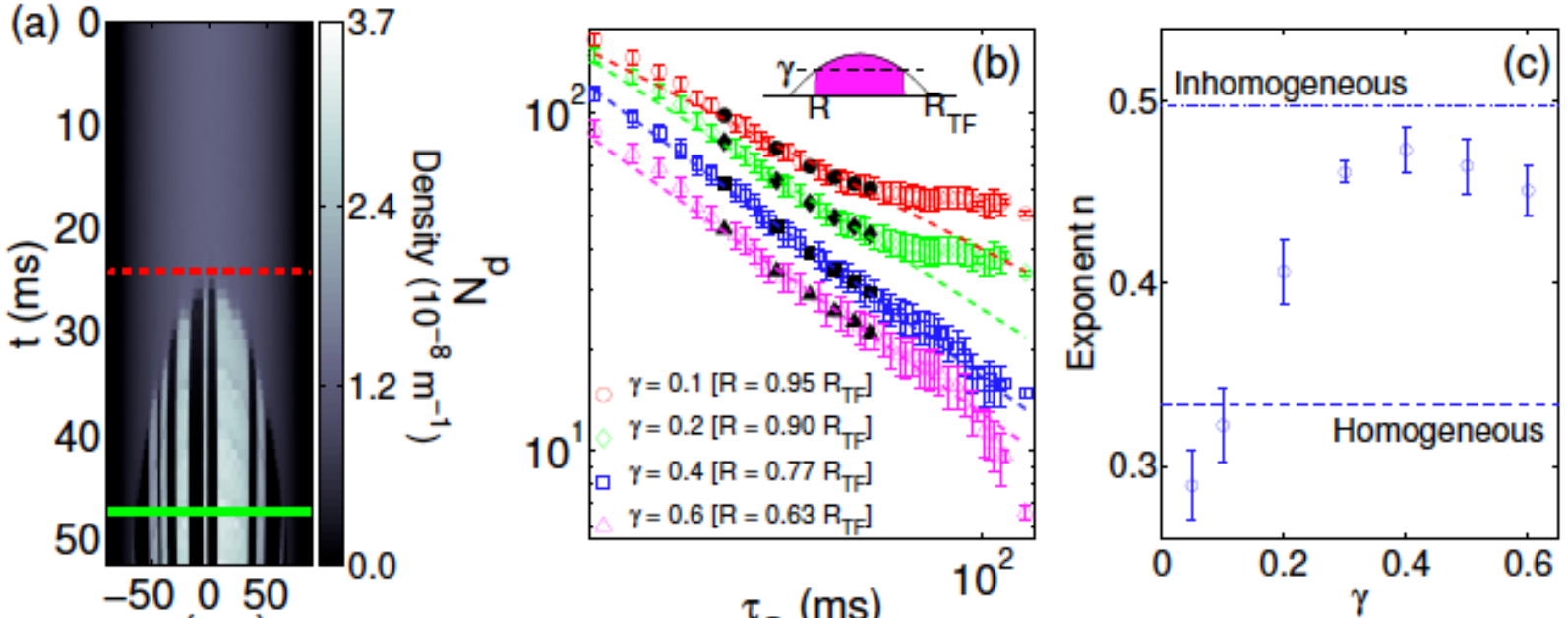
(a)
t (ms)
Density (10^{-8} m^{-1})
(b)
γ
R
R_{TF}
γ = 0.1 [R = 0.95 R_{TF}]
γ = 0.2 [R = 0.90 R_{TF}]
γ = 0.4 [R = 0.77 R_{TF}]
γ = 0.6 [R = 0.63 R_{TF}]
(c)
Inhomogeneous
Homogeneous
Exponent n
γ

Critical Dynamics of Decoherence

Ising chain driven through the phase transition(s) is an environment of a single qubit. We study decoherence factor.

B. Damski, H. T. Quan, WHZ
Phys. Rev. A83: 062104,2011

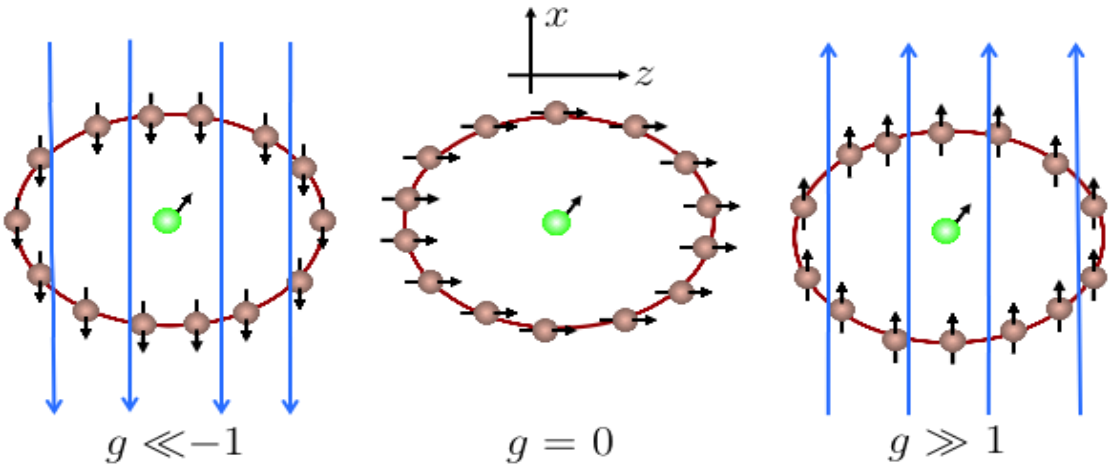

$$\hat{H}_{\mathcal{E}} = -\sum_{j=1}^{N} \sigma_j^x \sigma_{j+1}^x + g(t)\sigma_j^z$$

$$g(t) = 1 - t/\tau_Q,$$

$$\hat{H}_{\mathcal{SE}} = -\delta \sum_{j=1}^{N} \sigma_j^z \sigma_{\mathcal{S}}^z.$$

$$\hat{H} = \hat{H}_{\mathcal{E}} + \hat{H}_{\mathcal{SE}}.$$

$$|\psi(t=-\infty)\rangle = |GS(t=-\infty)\rangle \otimes (c_+ |\uparrow\rangle + c_- |\downarrow\rangle)$$

$$\begin{aligned} |\psi(t)\rangle &= \hat{T} e^{-i\int_{-\infty}^{t} dt\, \hat{H}(g(t))} |\psi(t=-\infty)\rangle \\ &= c_+ |\uparrow\rangle \otimes \hat{T} e^{-i\int_{-\infty}^{t} dt \hat{H}_{\mathcal{E}}(g(t)+\delta)} |GS(t=-\infty)\rangle \\ &+ c_- |\downarrow\rangle \otimes \hat{T} e^{-i\int_{-\infty}^{t} dt \hat{H}_{\mathcal{E}}(g(t)-\delta)} |GS(t=-\infty)\rangle \end{aligned}$$

$$\rho_{\mathcal{S}}(t) = \mathrm{Tr}_{\mathcal{E}} |\psi(t)\rangle\langle\psi(t)| = \begin{pmatrix} |c_+|^2 & c_+^* c_- d(t) \\ c_+ c_-^* d^*(t) & |c_-|^2 \end{pmatrix}$$

A straightforward calculation then shows that

$$\begin{aligned}
|\psi(t)\rangle &= \hat{T} e^{-i\int_{-\infty}^{t} dt\, \hat{H}(g(t))} |\psi(t=-\infty)\rangle \\
&= c_+ |\uparrow\rangle \otimes \hat{T} e^{-i\int_{-\infty}^{t} dt \hat{H}_{\mathcal{E}}(g(t)+\delta)} |GS(t=-\infty)\rangle \\
&+ c_- |\downarrow\rangle \otimes \hat{T} e^{-i\int_{-\infty}^{t} dt \hat{H}_{\mathcal{E}}(g(t)-\delta)} |GS(t=-\infty)\rangle \\
&= c_+ |\uparrow\rangle \otimes |\varphi_+(t)\rangle + c_- |\downarrow\rangle \otimes |\varphi_-(t)\rangle, \qquad (6)
\end{aligned}$$

where $\hat{T}$ is the time-ordering operator, and evolution of the environmental states coupled to up-down qubit states is given by

$$i\frac{\partial}{\partial t} |\varphi_\pm(t)\rangle = \hat{H}_{\mathcal{E}}(g(t) \pm \delta) |\varphi_\pm(t)\rangle . \qquad (7)$$

Therefore, evolution of the system depends on dynamics of two Ising branches evolving in an effective magnetic field given by $g(t) \pm \delta$.

The reduced density matrix of the qubit in the $\{|\uparrow\rangle, |\downarrow\rangle\}$ basis reads

$$\rho_{\mathcal{S}}(t) = \mathrm{Tr}_{\mathcal{E}} |\psi(t)\rangle\langle\psi(t)| = \begin{pmatrix} |c_+|^2 & c_+^* c_- d(t) \\ c_+ c_-^* d^*(t) & |c_-|^2 \end{pmatrix},$$

where $d(t) = \langle\varphi_+(t)|\varphi_-(t)\rangle$ is the decoherence factor. We study its squared modulus,

$$D = |d(t)|^2 = |\langle\varphi_+(t)|\varphi_-(t)\rangle|^2, \qquad (8)$$

also known as the decoherence factor; we follow this nomenclature below. When $D = 1$, the qubit is in a pure state, but when $D = 0$ it is completely decohered.

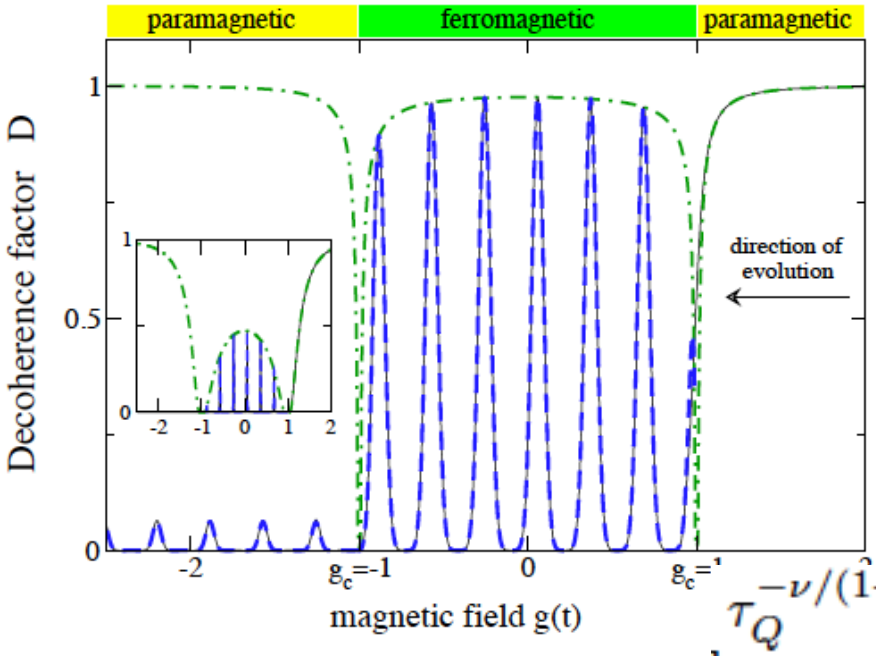

FIG. 2: (color online) Decoherence during a quench: a quasi-periodic regime between the critical points. Black solid line is a numerical solution. Our analytical approximations are superimposed on it as a blue dashed line: (20) for $g(t) \in (-1, 1)$ and (23) for $g(t) < -1$. The green dashed-dotted line is the adiabatic result equivalent to ground state fidelity ($\tau_Q \to \infty$ limit). Numerical solution almost perfectly overlaps with analytical results away from the critical points – $|g - g_c| > \hat{g}, \delta$. Them main plot shows that for moderate environment sizes – $N = 1000$ here – almost perfect revivals of coherence take place between the critical points, but coherence is virtually lost after driving the environment through the second critical point. The inset, prepared for $N = 30,000$, illustrates that for very large environments there is little coherence left after passing the first critical point and the qubit is completely decohered after crossing the second critical point. Interestingly, the ground state fidelity provides the envelope for the revivals between the critical points. We used here $\delta = 10^{-2}$ and $\tau_Q = 250$.

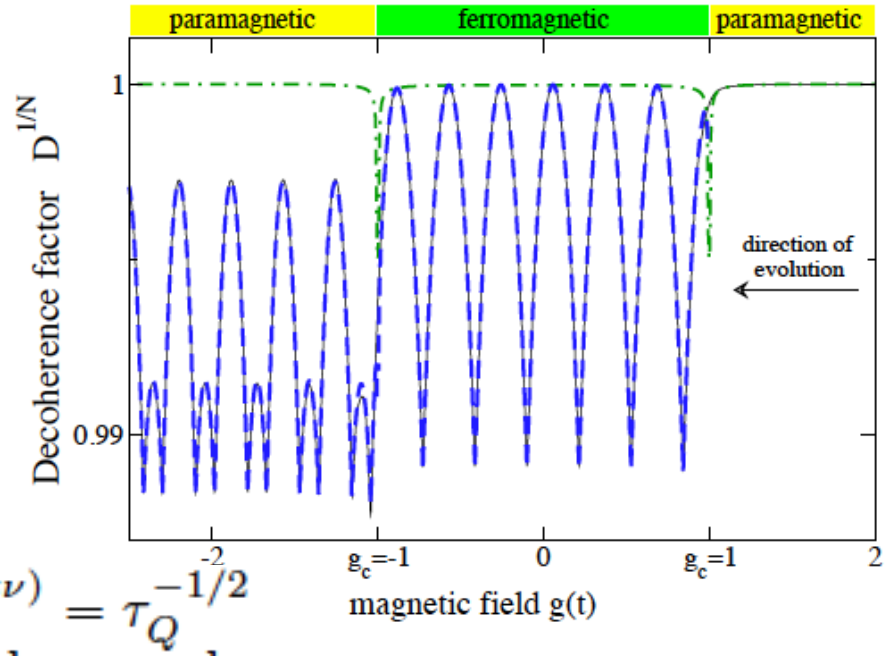

$$\tau_Q^{-\nu/(1+z\nu)} = \tau_Q^{-1/2}$$

FIG. 3: (color online) Same as in Fig. 2, except we consider here N-th root of the decoherence factor D – decoherence per spin – illustrating details of decoherence dynamics in the large N limit. Data from Fig. 2 is used to make this plot: $N = 1000$ and $N = 30,000$ data sets provide indistinguishable $D^{1/N}$ on the scales explored in this plot.

$$D \approx \exp\left(-\frac{N\delta^2}{4(1-g^2)}\right) \exp\left(-\frac{N}{2\pi}\frac{f[\phi(t)]}{\sqrt{\tau_Q}}\right), \qquad (20)$$

where $f[\phi] = -\frac{1}{\sqrt{2\pi}} \int_0^\infty ds \ln[1 - 4(e^{-s^2} - e^{-2s^2}) \sin^2 \phi]$ and $\phi \approx 4t\delta$. The first factor above is again ground

the modes centered around

$$k_m = \sqrt{\frac{\ln 2}{2\pi}} \frac{1}{\sqrt{\tau_Q}}$$

contribute most to non-equilibrium decoherence

Adiabatic crossing

of a

quantum phase transition

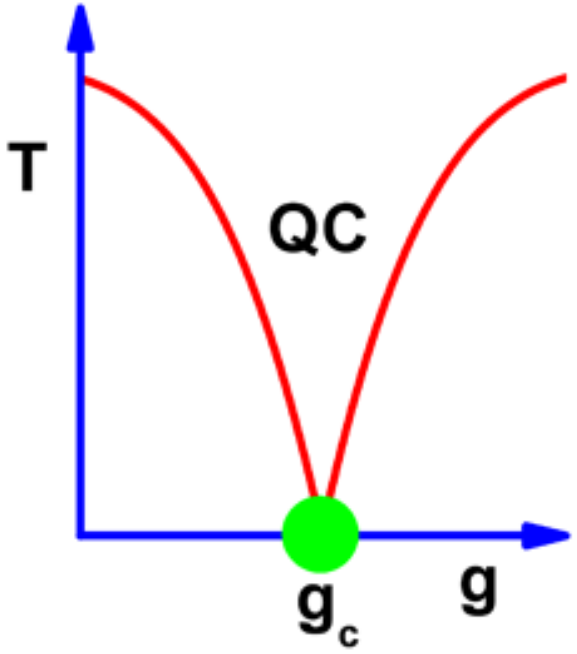

A. del Campo, M. M. Rams, W. H. Zurek, PRL, arXiv:1206.2670

Idea

Take a time-dependent Hamiltonian with instantaneous eigenstates:

$$\hat{H}_0(t)|n(t)\rangle = E_n(t)|n(t)\rangle$$

Write the adiabatic approximation

$$|\psi_n(t)\rangle = \exp\left\{-\frac{\mathrm{i}}{\hbar}\int_0^t \mathrm{d}t' E_n(t') - \int_0^t \mathrm{d}t' \langle n(t')|\partial_{t'} n(t')\rangle\right\}|n(t)\rangle$$

Look for a Hamiltonian for which the adiabatic approximation is exact

$$\mathrm{i}\hbar\partial_t|\psi_n(t)\rangle = \hat{H}(t)|\psi_n(t)\rangle$$

It follows that $\hat{H}(t) = \hat{H}_0(t) + \hat{H}_1(t)$

Auxiliary term: $\hat{H}_1(t) = \mathrm{i}\hbar\sum_{m\neq n}\sum \frac{|m\rangle\langle m|\partial_t \hat{H}_0|n\rangle\langle n|}{E_n - E_m}$

Demirplak & Rice 2003, 2005; M. V. Berry 2009

Quantum critical systems

Family of quasi-free fermion models

$$\mathscr{H}_0 = \sum_{\mathbf{k}} \psi_{\mathbf{k}}^{\dagger} \left[\vec{a}_{\mathbf{k}}(\lambda(t)) \cdot \vec{\sigma}_{\mathbf{k}}\right] \psi_{\mathbf{k}}$$

$$\vec{\sigma}_{\mathbf{k}} = (\sigma_{\mathbf{k}}^{x}, \sigma_{\mathbf{k}}^{y}, \sigma_{\mathbf{k}}^{z})$$

$$\psi_{\mathbf{k}}^{\dagger} = (c_{\mathbf{k},1}^{\dagger}, c_{\mathbf{k},2}^{\dagger})$$

Model dependent vector $\vec{a}_{\mathbf{k}}(\lambda) = (a_{\mathbf{k}}^{x}(\lambda), a_{\mathbf{k}}^{y}(\lambda), a_{\mathbf{k}}^{z}(\lambda))$

Examples: Ising, XY in 1D, Kitaev model in 1D, 2D

Auxiliary Hamiltonian in Fourier space

$$\mathscr{H}_1 = \lambda'(t) \sum_{\mathbf{k}} \frac{1}{2|\vec{a}_{\mathbf{k}}(\lambda)|^2} \psi_{\mathbf{k}}^{\dagger} \left[(\vec{a}_{\mathbf{k}}(\lambda) \times \partial_{\lambda} \vec{a}_{\mathbf{k}}(\lambda)) \cdot \vec{\sigma}_{\mathbf{k}}\right] \psi_{\mathbf{k}}$$

Long-range time-dependent interactions. Example: Ising model

$$\mathscr{H}_1 = -g'(t) \left[\sum_{m=1}^{N/2-1} h_m(g) \mathscr{H}_1^{[m]} + \frac{1}{2} h_{N/2}(g) \mathscr{H}_1^{[N/2]}\right] \qquad h_m = \frac{1}{8} \begin{cases} g^{m-1} & \text{for } |g| < 1 \\ g^{-m-1} & \text{for } |g| > 1 \end{cases}$$

$$\mathscr{H}_1^{[m]} = \sum_{n=1}^{N} \left(\sigma_n^x \sigma_{n+1}^z \cdots \sigma_{n+m-1}^z \sigma_{n+m}^y + \sigma_n^y \sigma_{n+1}^z \cdots \sigma_{n+m-1}^z \sigma_{n+m}^x\right)$$

A. del Campo, M. M. Rams, W. H. Zurek, PRL, arXiv:1206.2670

Precluding the KZM scaling

A. del Campo, M. M. Rams, WHZ, PRL

arXiv:1206.2670

Transverse field: linear quench of through critical point $g(t) = g_c - \upsilon t$

Truncated Auxiliary Hamiltonian $\tilde{\mathscr{H}}_1(M) = \upsilon \sum_{m=1}^{M} s_m h_m(g) \mathscr{H}_1^{[m]}$

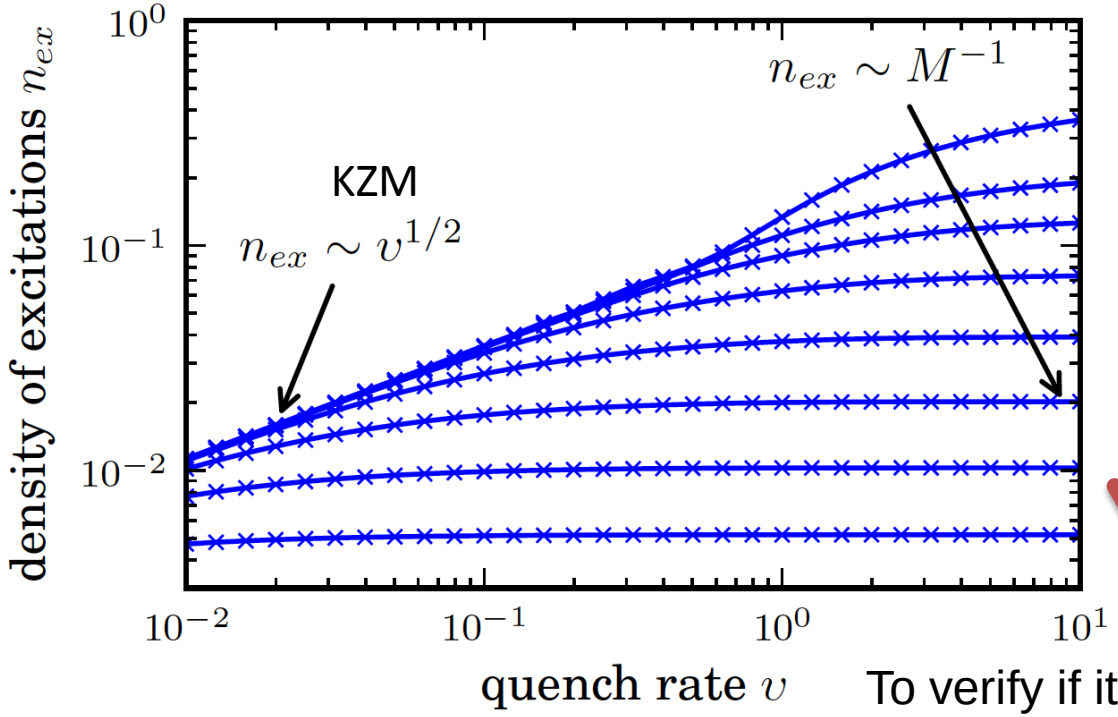

Range of interactions M

To verify if it works:

arXiv:1007.3294 **Testing quantum adiabaticity with quench echo**

H. T. Quan, W. H. Zurek

New Journal of Physics, 12 (2010) 093025

Topological Schrödinger Cat in a Quantum Ising Chain

Non-local superposition of "kinks":

$$|\cdots\uparrow\uparrow\uparrow\underbrace{\downarrow\downarrow\cdots\downarrow\downarrow}_{L}\downarrow\downarrow\downarrow\cdots\rangle$$
$$+|\cdots\uparrow\uparrow\uparrow\underbrace{\uparrow\uparrow\cdots\uparrow\uparrow}_{L}\downarrow\downarrow\downarrow\cdots\rangle$$

arXiv:1106.2823 Topological Schrödinger cats… J. Dziarmaga, WHZ, M. Zwolak: Nature Physics 8, 49-54 (2012)

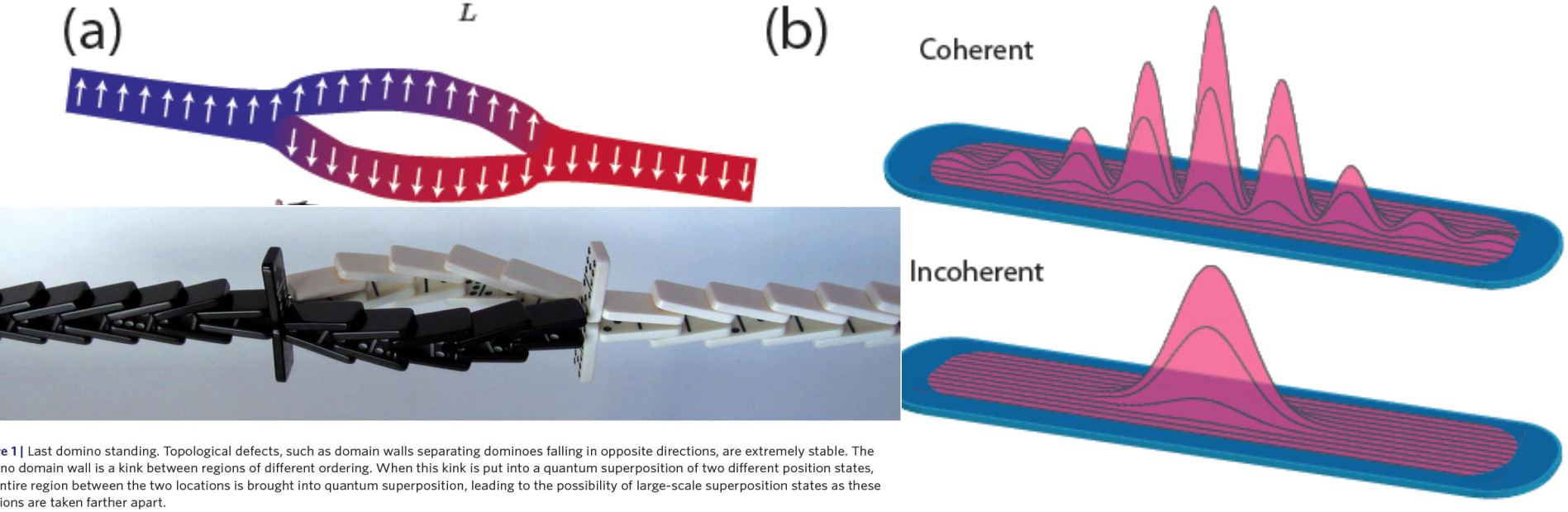

e 1 | Last domino standing. Topological defects, such as domain walls separating dominoes falling in opposite directions, are extremely stable. The no domain wall is a kink between regions of different ordering. When this kink is put into a quantum superposition of two different position states, ntire region between the two locations is brought into quantum superposition, leading to the possibility of large-scale superposition states as these ions are taken farther apart.

Figure 1: A Schrödinger kink in a quantum Ising chain. (a) A topological defect in a non-local superposition and (b) The analogue of a double-slit experiment. A double-well potential (left) is used to create a topological defect, such as a domain wall, superimposed in two locations (here, defect is represented by its probability distribution in space). To carry out the double slit experiment, the two potential wells are eliminated, allowing the defect to move. In isolation, the two wavepackets emerging from the "slits" interfere creating fringes of high and low probability for the location of the kink. However, when the system interacts with the environment, such a superposition will decohere at rate proportional to the distance L – the unzipped part of the chain shown in (a), which corresponds to the size of the Schrödinger kink – resulting in a classical distribution for the defect.

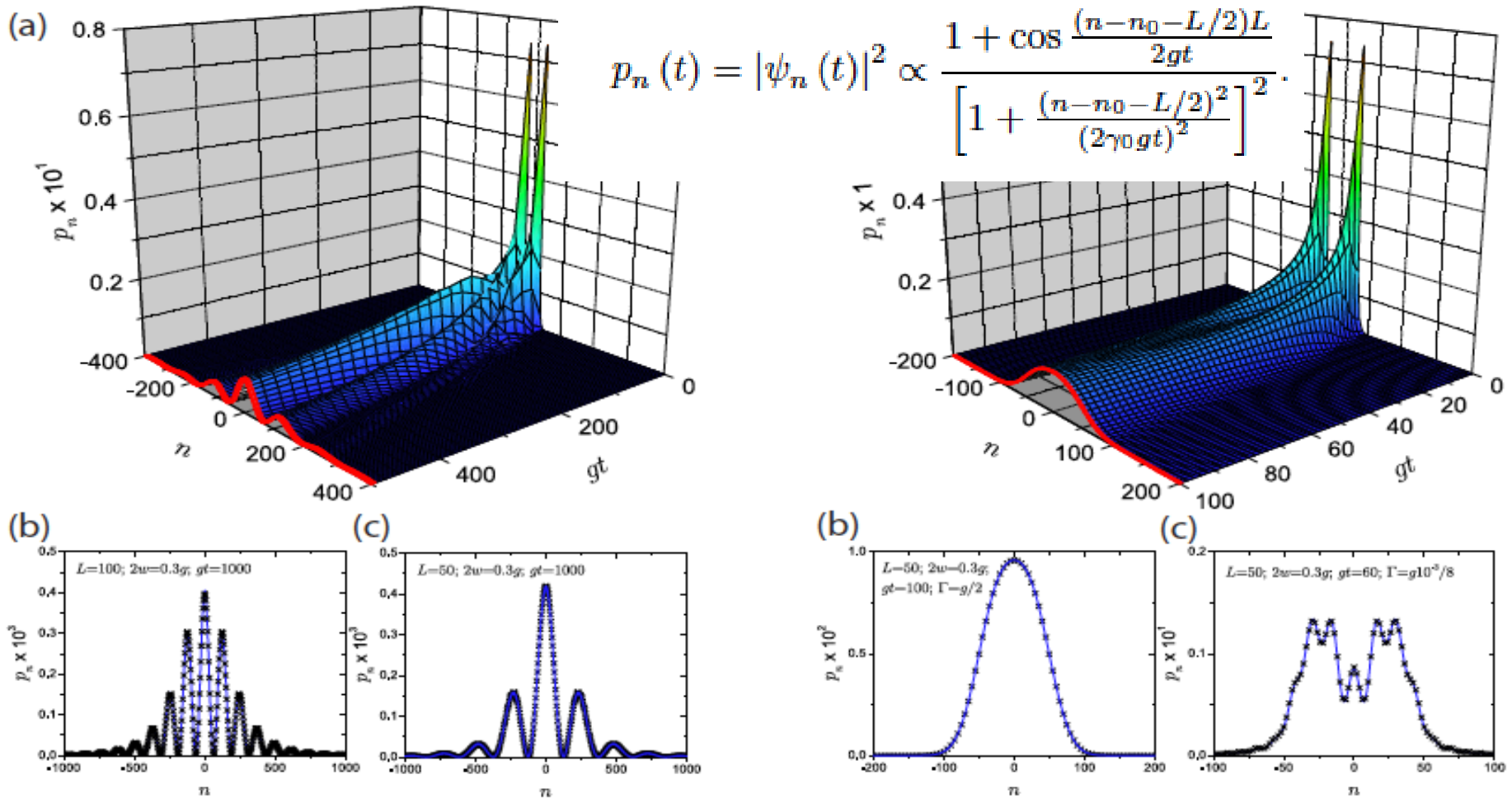

Figure 2: Interference patterns after a Schrödinger kink is released. (a) Time evolution of the Schrödinger kink for $L = 50$ and $2w = 0.3g$ results in an interference pattern (highlighted in red at the final time). (b) Interference pattern in the long time limit ($gt = 1000$) for $L = 100$ and $2w = 0.3g$. The exact data is shown as black crosses and the expression, equation (4), is shown as the blue line. (c) Interference pattern in the long time limit ($gt = 1000$) for $L = 50$ and $2w = 0.3g$. The exact data is shown as black crosses and equation (4) is shown as the blue line. As the initial superimposed kink is shortened, the interference pattern diminishes.

Figure 3: A Schrödinger kink evolved in the presence of decoherence. (a) Time evolution for strong decoherence ($\Gamma = g/2$), $L = 50$, and $2w = 0.3g$, where the Schrödinger kink evolves into a (b) Gaussian mixture of locations (highlighted in red in (a)) at a later time, $gt = 100$ (the black crosses are the exact data and the blue curve is the solution to the diffusion equation). (c) Under weak decoherence ($\Gamma = g10^{-3}/8$), the superposition is still visible at intermediate times, but the decoherence smooths out the fringes (the black crosses are the exact data and the blue curve is the pure state solution convoluted with a Lorentzian).

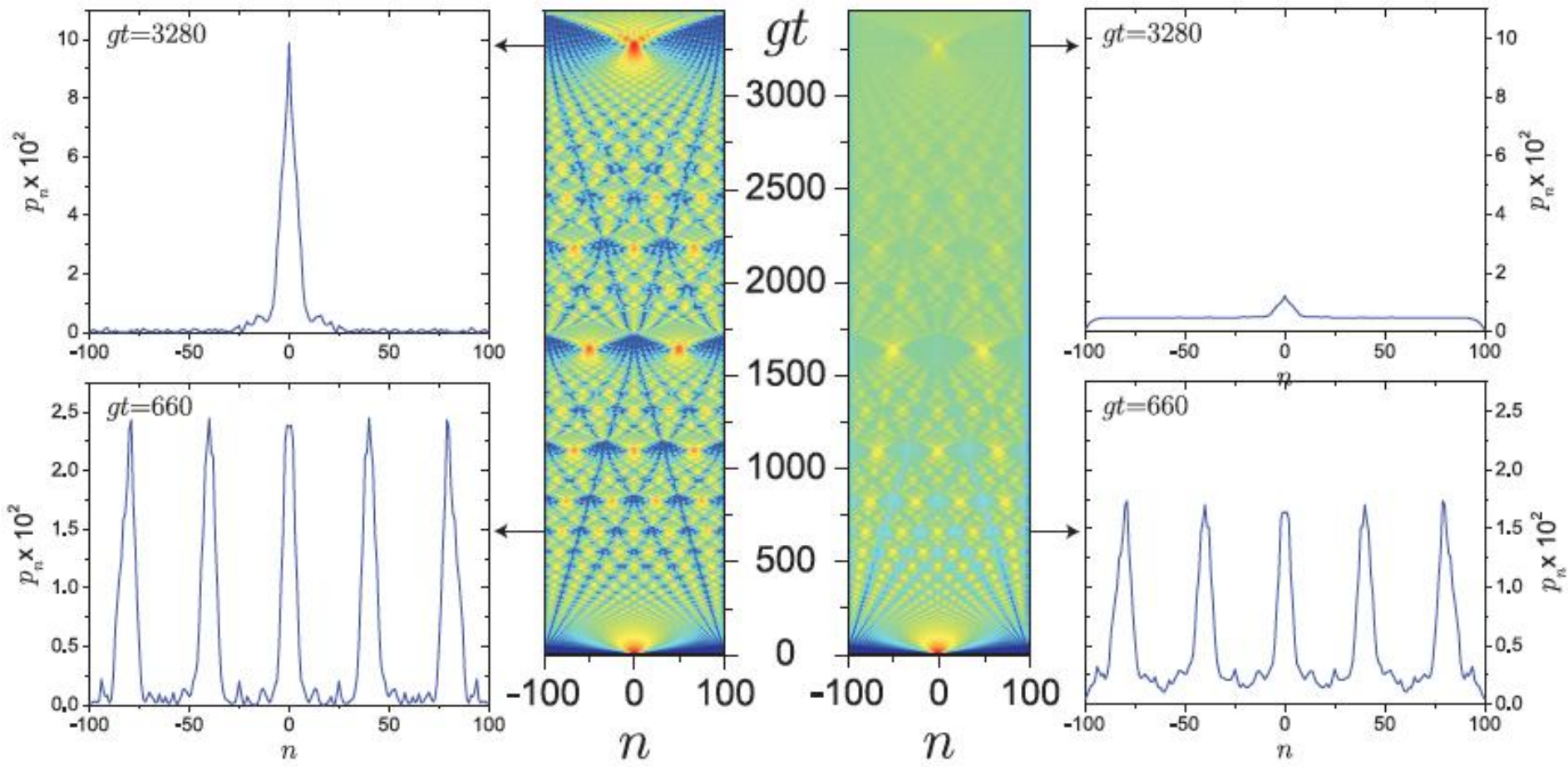

Figure 4: A single kink evolved on a finite lattice with and without decoherence. (Left) Time evolution without decoherence on an $L = 201$ site lattice and $2w = 0.5g$. The kink travels outward on the lattice and after reflecting off the boundaries, it starts to interfere with itself. The leftmost panels show the self interference at two particular times. (Right) The same simulation except in the presence of weak decoherence ($\Gamma = 3g \times 10^{-6}$). The kink can still interfere with itself, but eventually the decoherence will set in. In the supplemental information, we show movies of the development of this interference pattern for different values of w.

Quench from Mott Insulator to Superfluid

Jacek Dziarmaga,[1] Marek Tylutki,[1] and Wojciech H. Zurek[2]

We study a linear ramp of the nearest-neighbor tunneling rate in the Bose-Hubbard model driving the system from the Mott insulator state into the superfluid phase. We employ the truncated Wigner approximation to simulate linear quenches of a uniform system in 1...3 dimensions, and in a harmonic trap in 3 dimensions. In all these setups the excitation energy decays like one over third root of the quench time. The $-1/3$ scaling is explained by an impulse-adiabatic approximation - a variant of the Kibble-Zurek mechanism - describing a crossover from non-adiabatic to adiabatic evolution when the system begins to keep pace with the increasing tunneling rate.

$$H = -J \sum_{\langle \mathbf{s_1}, \mathbf{s_2} \rangle} a^\dagger_{\mathbf{s_1}} a_{\mathbf{s_2}} + \sum_{\mathbf{s}} \left(\frac{1}{2n} a^\dagger_{\mathbf{s}} a^\dagger_{\mathbf{s}} a_{\mathbf{s}} a_{\mathbf{s}} + V_{\mathbf{s}} a^\dagger_{\mathbf{s}} a_{\mathbf{s}} \right)$$

When $n \gg 1$ we can replace annihilation operators $a_{\mathbf{s}}$ by a complex field $\phi_{\mathbf{s}}$, $a_{\mathbf{s}} \approx \sqrt{n}\phi_{\mathbf{s}}$, normalized as $\sum_{\mathbf{s}} |\phi_{\mathbf{s}}|^2 = L^D$ and evolving with the Gross-Pitaevskii equation (GPE)

$$i\frac{d\phi_{\mathbf{s}}}{dt} = -J\nabla^2\phi_{\mathbf{s}} + \left(|\phi_{\mathbf{s}}|^2 - 1\right)\phi_{\mathbf{s}} \ , \qquad (6)$$

see Refs. [13]. Here

$$\nabla^2\phi_{\mathbf{s}} = \sum_{\alpha=1}^{D} \left(\phi_{\mathbf{s}+\mathbf{e}_\alpha} - 2\phi_{\mathbf{s}} + \phi_{\mathbf{s}-\mathbf{e}_\alpha}\right) \qquad (7)$$

We drive the system by a linear quench

$$J(t) = t/\tau_Q \ ,$$

starting in the Mott ground state at $J = 0$,

$$|n, n, n, \ldots, n\rangle \ ,$$

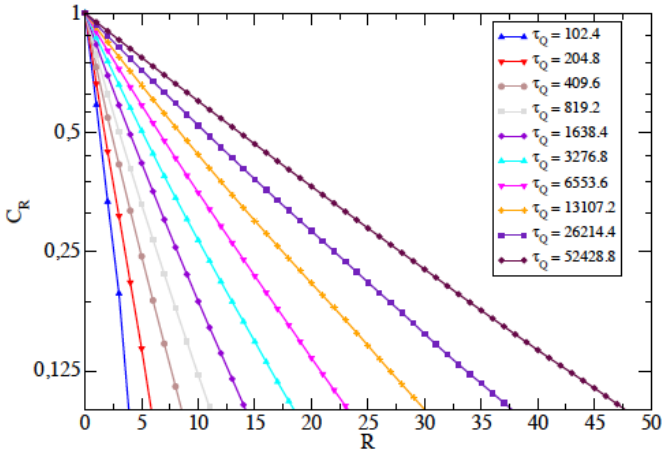

FIG. 6. Correlation functions C_R in 1D at $J = 0.1$ for different quench times τ_Q. The functions are exponential, as expected in a thermal state in the adiabatic stage of the evolution. Their correlation length scales like $\xi \sim \tau_Q^{\alpha}$ with the best fit $\alpha = 0.329$ close to the predicted 1/3.

We drive the system by a linear quench

$$J(t) \;=\; t/\tau_Q \;,$$

starting in the Mott ground state at $J = 0$,

$$|n, n, n, \ldots, n\rangle \;,$$

$$C_R \;=\; \frac{1}{n}\langle a^{\dagger}_{\vec{s}} a_{\vec{s}+\vec{R}}\rangle \;=\; \exp\left(-R/\xi\right)$$

$$\xi \;\approx\; \frac{4J}{T} \;\simeq\; \frac{J^{1/2}}{\hat{J}^{1/2}} \;\simeq\; J^{1/2}\tau_Q^{1/3}$$

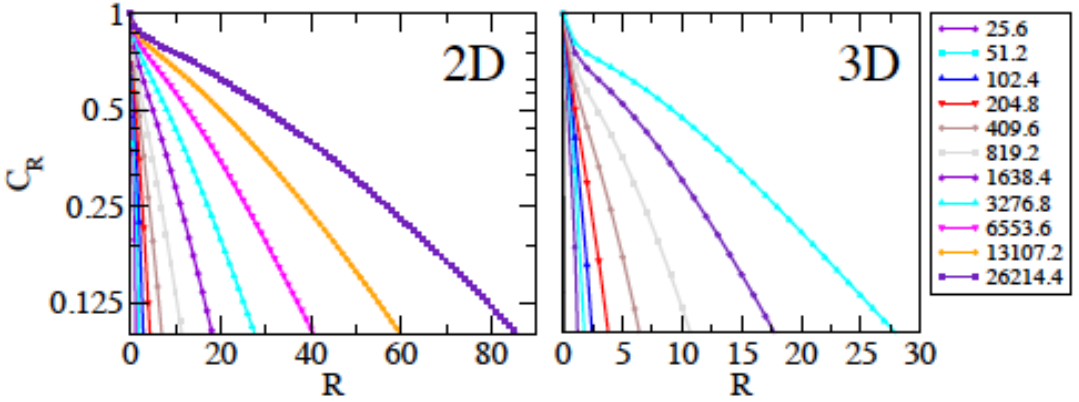

FIG. 7. Long-range tail of the correlation functions C_R in 2D and 3D at $J = 0.1$ for different quench times τ_Q. They are in the adiabatic stage, in the sense that local observables have equilibrated, but they have not had enough time to develop the infinite-range (quasi-)long-range order expected in the low temperature phase. Instead the correlations have finite range limited by a finite rate at which they can spread across the system. The range grows with τ_Q faster than $\tau_Q^{1/2}$.

Vortices in 2D and 3D

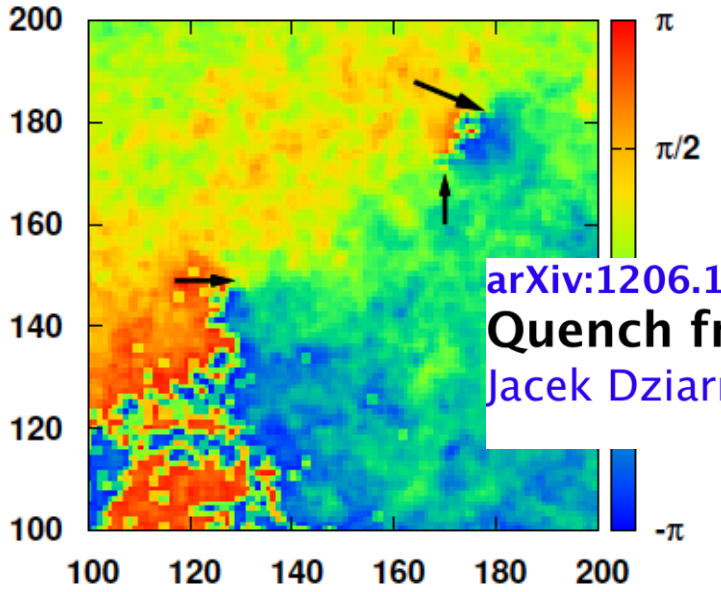

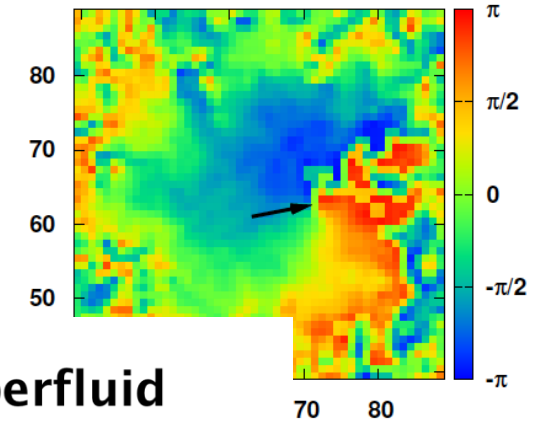

arXiv:1206.1067

Quench from Mott Insulator to Superfluid

Jacek Dziarmaga, Marek Tylutki, Wojciech H. Zurek